AN INVESTIGATION OF THE NON-LINEAR DYNAMICS OF A
PROTON BEAM USING THE HYDRODYNAMIC METHOD*

A.J. Davies
European Organisation for Nuclear Research
Geneva, Switzerland
Dpt. of Physics, University of Swansea
Swansea, Great Britain

ABSTRACT

A study has been made of the dynamics of the proton beam in the pre-injector region of the CERN Linac where the beam has approximate rotational symmetry. It is shown that the hydrodynamic approach (allowing for particle overtaking and the non-linear effects of space charge) can give a satisfactory description of the beam dynamics.

The numerical programme has been designed to operate in a semi-interactive manner, via a remote cathode ray display, with a CDC 6600 computer and has proved a powerful tool in investigating the properties of the proton beam. Typical results are presented and discussed.

Introduction

In a previous article[1] the author has described a method for following the transverse motion of rotationally symmetric charged particle beams in the presence of non-linear space charge fields. It was shown how it was possible to trace the mean motion of the beam and its boundary in the phase plane r (radius) - r' (radial velocity). Allowance was made for linear external focussing or defocussing fields and also for acceleration in the axial, z, direction.

In the present work the method is extended (a) to trace the motion of an arbitrary section of the initial hyperellipsoid in the xx'yy' transverse phase space, and (b) to allow for the radial and axial fields occuring when the beam is travelling through an electrode system having the Pierce[2] geometry. The study of the latter case is of particular interest in the design of the accelerating column of a pre-injector as it may be possible to reduce the transverse emittance growth of the beam by using such a geometry.

The numerical programmes take only a small amount of computing time and thus have been designed to be used in a semi-interactive manner with the CDC 6600 computer at CERN. The results are produced in graphical form and are device independent so that they may be displayed on a cathode ray tube or be output on a lineprinter, a sequential mechanical plotter, or an electron beam recording device (microfilm).

* Paper submitted to the 1970 Proton Linear Accelerator Conference, NAL, Batavia (U.S.A)

Method of Integration

For zero emittance beams having rotational symmetry the equations describing the radial motion of the beam are

$$\frac{D\rho}{Dt} + \rho \frac{\partial u_r}{\partial r} = 0 \tag{1}$$

and

$$m \frac{Du_r}{Dt} = e E_r \tag{2}$$

where ρ is the density at a point, u_r and E_r are the r components of the velocity and electric field and D/Dt denotes differentiation in a frame of reference following the motion of the element of the beam under consideration. Macroscopic rotational motion of the beam is neglected and the beam divergence is taken to be small so that longitudinal effects can be neglected.

The initial condition of the beam will be described by a line (the so-called "zero emittance line") defining u_r as a function of r in the phase plane rr' (e.g. curve (i) in Fig. 1), and an arbitrary distribution, $\rho(r)$, of charge in the radial direction.

The subsequent motion of the beam may now be followed by integrating the hydrodynamic equations (1) and (2) and does not involve any difficulty unless particle overtaking occurs when $\rho(r)$ can have singularities at some values of r. In [1] the author pointed out that this difficulty could be overcome quite simply by computing ρ as a function of s, the distance along the zero emittance line, instead of a function of r. Since particle overtaking cannot occur along this line (i.e. a particle having an initial value of s less than that of another particle will continue to have a smaller value) a continuous density distribution $\rho(s)$ will always remain continuous.

The space charge field at a point P a distance r_1 from the axis is given by

$$2q(r_1)/r_1 \tag{3}$$

where $q(r_1)$ is the quantity of charge per unit length of the beam inside r_1 and may be found by projecting the charge distribution along the zero emittance line on to the r axis. Thus $q(r_1)$ in Fig. 1 is given by the sum of the charge between the origin and A and along the arc BCD.

If we now consider an arbitrary point, P, on the zero emittance line, its radial coordinate and velocity are already specified together with any external fields, and the space charge field may by found from (3) so that we may integrate (1) and (2) along the characteristic curve following the motion of P in the plane rr'. In this manner the position of the zero emittance line is determined at any subsequent time together with the charge distribution along this line.

Now in [1] we showed that for beams of finite but reasonably small emittance the densities and velocities computed from (1) and (2) represent to a good approximation the mean motion of the beam and that, furthermore, the space charge force at an arbitrary point of the beam in phase space could be taken as that computed from the mean motion. Thus, having solved (1) and (2), we have, in fact, defined the space charge force at any point in the beam's history.

If we now wish to trace the motion of any contour or section of the initial hyperellipsoid we have only to choose representative points defining this contour or section and to compute their position at any subsequent time taking the space charge force on any particle to be that given by the mean motion of the beam.

The Pierce Geometry

One may take approximate account of the effects of acceleration of the beam in the axial direction by assuming that the sole effect of the resulting increase in axial velocity $v_z(t)$ is to dilute the space charge in the ratio $v_z(0)/v_z(t)$. As a special case one may consider the Pierce geometry[2] which has the property that a uniform, zero emittance, beam having a current density J, equal to that for which the electrodes were designed, will remain uniform and of constant radius.

The variation of potential in the z direction on the axis is given by

$$V(z,0) = Az^{4/3} \tag{4}$$

where

$$A = \left(\frac{9 \pi J}{\sqrt{2\varepsilon/300}} \right)^{2/3}$$

so that the axial accelerating field is

$$E_a(z,0) = \frac{4}{3} Az^{1/3} \tag{5}$$

ε is the ratio of charge to mass of the proton in e.s.u., $V(z,0)$ is in volts and J in amps/cm^2.

Since $V(z,0)$ is a smooth function of z we can find the potential near to the axis by expanding the potential as a Taylor series

$$V(z,r) = V(z,0) + \frac{1}{2} \frac{\partial^2 V(z,0)}{\partial r^2} \cdot r^2 + \frac{1}{24} \frac{\partial^4 V(z,0)}{\partial r^4} \cdot r^4 + \ldots \ldots \tag{6}$$

remembering that the system has axial symmetry. If we neglect terms beyond r^2 and use Laplace's equation

$$\frac{\partial^2 V(z,r)}{\partial z^2} + \frac{1}{r} \frac{\partial V(z,r)}{\partial r} + \frac{\partial^2 V(z,r)}{\partial r^2} = 0$$

we see that we may write

$$V(z,r) = V(z,0) - \frac{1}{4} \frac{\partial^2 V(z,0)}{\partial z^2} \cdot r^2 \tag{7}$$

and the radial field $E_r(z,r)$ is given by

$$E_r(z,r) = - \frac{r}{2} \frac{\partial^2 V(z,0)}{\partial z^2} = - \frac{2A}{q \, z^{2/3}} \cdot r \quad . \tag{8}$$

Thus the Pierce geometry imposes a continually varying accelerating field $E_a(z,0)$ in the axial direction and a continually varying linear focusing field in the r direction. We may therefore incorporate the effects of a Pierce geometry into the calculation by allowing for the axial acceleration derived from (5) and for the linear focusing force found from (8).

It might be thought that a more accurate approximation to the radial fields could be obtained by incorporating higher order terms in (6). This, however, will not improve the overall accuracy as may be seen from the following argument.

The Pierce geometry is designed so that a uniform beam of the requisite current density J will remain uniform and its radius will not alter. Now the space charge field in such a beam is given by (3) and writing this in terms of the current density J

$$E_r(z,\dot{r}) = \frac{2q(r)}{r} = \frac{2 \pi J}{\sqrt{2\varepsilon V(z,0)/300}} \cdot r$$

since J remains constant.

The radial field due to the Pierce structure is, from (8),

$$E_r(z,r) = - \frac{2}{q} \frac{A}{z^{2/3}} \cdot r = - \frac{2}{q} \frac{A^{3/2}}{\sqrt{V(z,0)}} \cdot r$$

$$= \frac{- 2 \pi J}{\sqrt{2\varepsilon V(z,0)/300}} \cdot r \quad ,$$

so that the radial fields exactly cancel and the beam will remain uniform and of constant radius. The calculation is thus more accurate than we could reasonably expect, the inaccuracies in the space charge calculation being compensated by neglecting the higher order terms in (6).

Display of Results

The numerical procedure written to follow the beam dynamics takes typically ten seconds of CDC 6600 CPU time to follow the beam for 100 time increments. Because of this comparatively short computing time it has proved feasible to write the computer programmes

in such a way that they can be used in a semi-interactive manner. Although the results can be output numerically they are also put in a form suitable for graphical display using a device independent set of plotting routines[3].

In analysing any particular beam transport system, the programme and data files are assembled on a CDC 3100 computer via a remote CRT display and are then transmitted to the CDC 6600 - the graphical display file being returned at the end of the computation. The particle trajectories, the positions of the zero emittance line, beam boundary, etc., may then be examined on the cathode ray display. If the results for a particular section of the system are satisfactory the results are at present sent for plotting on a Calcomp incremental plotter but in the near future will be recorded on microfilm using an electron beam recording device. The computation may then be continued for the next section of the transport system or the current section can be repeated, if necessary, using different values for the various parameters.

The typical turn round time is of the order of three minutes for 30 seconds of 6600 CPU time so that in a single session of, say, two or three hours it is possible to design a transport or optical system having seen the effect of altering many of the design parameters.

Results

In the study of the beam dynamics two sets of results have proved to be of great use - (a) the trajectories of particles following the mean motion of the beam and -(b) the variation of the zero emittance line with time. To illustrate this we show in Figs. 2 to 4 the trajectories of a proton beam in the presence of a linear focusing field.

If the beam is uniform and the external field exactly compensates the space charge field then the particle trajectories would be straight lines parallel to the z axis. In Fig. 2 the initial conditions are such that a uniform beam is at a waist. The subsequent trajectories oscillate with constant frequency and remain in phase. In Fig. 3 the initial density distribution is Gaussian, i.e.

$$\rho(r) = \rho(0) \ e^{-r^2/2\sigma^2 R} \tag{9}$$

with $\sigma = \sqrt{2}$ and the resultant field is zero at the beam edge. Here we note that the trajectories are straight lines at the edge and on the axis, but due to the non-linearity in the space charge field, there is a resultant force on the particles at intermediate radii and thus the trajectories oscillate. Since the degree of non-linearity is small the particles remain in phase and the period of oscillation is the same as in Fig. 2.

In Fig. 4 the initial Gaussian distribution has $\jmath = \dfrac{1}{2.5 \sqrt{2}}$ so that there is a large degree of non-linearity present. We note that after about 1 metre particle overtaking starts to occur and that the beam effectively splits into two parts, one part oscillating in a stable manner with approximately the same frequency as in Fig. 2 but gradually getting out of phase and a second, outer, part which oscillates wildly - repeatedly passing through the axis.

The motion of the zero emittance line corresponding to Figs. 2 and 3 is easily visualised, and Fig. 5 shows the zero emittance line up to 4 metres in the last case considered above. We see clearly how the beam is beginning to filament.

The zero emittance line is defined by typical points at the initial instant whose motion is subsequently traced. It has proved useful to choose these points so that equal quantities of charge are enclosed between adjacent points along the line. If the position of each of these points is plotted then the linear density of these points will give a very good idea of the distribution of the beam charge in the phase plane rr'. This has proved particularly useful when the results are displayed on a cathode ray tube.

In Fig. 6 to Fig. 8 we show how the motion of sections of the initial hyper-ellipsoid in the transverse xx'yy' phase plane may be followed. The boundary of this hyperellipsoid will be defined by an equation of the form

$$\frac{x^2 + y^2}{a^2} + \frac{x'^2 + y'^2}{b^2} = 1$$

where a and b are the axes of the ellipsoid.

In Fig. 6 we have plotted the boundary of the beam in the xx' plane i.e.

$$y = y' = 0 \qquad \frac{x^2}{a^2} + \frac{x'^2}{b^2} = 1 \tag{10}$$

together with the contour in this plane which encloses 50% of the beam charge when this is projected on to the xx' plane. This contour will be the ellipse

$$y = y' = 0 \qquad \frac{x^2}{a^2} + \frac{x'^2}{b^2} = \frac{1}{k^2} \quad , \text{ say } (k > 1) \; . \tag{11}$$

We also consider the following three other sections of the hyperellipsoid which, initially, coincide with this contour when projected

$$y' = 0 \; , \quad y = a\sqrt{1 - \frac{1}{k^2}} \; , \quad \frac{x^2}{a^2} + \frac{x'^2}{b^2} = \frac{1}{k^2} \qquad ; \tag{12}$$

$$y = 0 \; , \quad y' = b\sqrt{1 - \frac{1}{k^2}} \; , \quad \frac{x^2}{a^2} + \frac{x'^2}{b^2} = \frac{1}{k^2} \qquad ; \tag{13}$$

and

$$y = \frac{a}{2}\sqrt{1 - \frac{1}{k^2}} \quad , \quad y' = \frac{3}{4} \cdot b \cdot \sqrt{1 - \frac{1}{k^2}} \quad , \quad \frac{x^2}{a^2} + \frac{x'^2}{b^2} = \frac{1}{k^2} \quad . \tag{14}$$

If the beam is uniform, so that the space increases linearly with radius, then it is easy to show that the contour (11) and the projections of the sections corresponding to (12) to (14) will coincide not only at the initial instant but throughout the motion of the beam. Thus the contour arising from (11) will always enclose 50% of the beam charge and, since it is of constant area due to Poincaré invariance, the emittance of the beam will be conserved in projection as well as in section.

This is not the case, however, when the beam is non-uniform so that the space charge force is non-linear. Fig. 7 shows the various projections and sections for an initially Gaussian beam which has drifted .5 metre, and Fig. 8 shows the corresponding results when a linear external field is applied so as to neutralise the space charge field at the edge of the beam. We see quite clearly the twisting of the hypervolume and note that the projections of the sections corresponding to (12) to (14) do not coincide when projected thus leading to an effective emittance growth in projection. The results obtained are a good illustration of the effects proposed by C.S. Taylor[4].

The Pierce electrode geometry is designed for a uniform beam of a specified current density. In the advance design study of the proposed 1.5 MeV pre-injector at CERN it was therefore of interest to investigate the effect of (a) varying the beam current, keeping the density uniform, and of (b) varying the density distribution with the beam current equal to the designed value – the results obtained then being compared with those corresponding to a conventional, constant gradient, accelerating tube.

Fig. 9 shows the particle trajectories computed for a uniform proton beam for various beam currents. We see that even with quite large variations in beam current the divergence is still quite small at 1.5 MeV.

Fig. 10 demonstrates the effect of various density distributions on the motion of the zero emittance line. We see that if the density falls off sharply with radius then it is possible for very large aberrations (indicated by the bending of the line) to be introduced. The maximum field gradient encountered in the Pierce geometry for this set of parameters is 7.6 MeV/metre and we display in Fig. 11 the zero emittance lines obtained for a conventional accelerating column with a potential gradient equal to this value.

We see that the beam divergence is larger than in Fig. 10 – the aberration, however, is much reduced. It is therefore interesting to note that the Pierce structure

has the advantage of keeping the beam divergence to a minimum but it does tend to introduce rather larger aberrations than a conventional column. We must remember, however, that on leaving the column the beam will enter a triplet lens and the larger the beam radius and divergence the bigger will be the aberrations introduced by the lens. In any particular case, therefore, we must compare the aberrations introduced in the column and the triplet before deciding on the accelerating structure to be used. In the case of the CERN pre-injector it is possible to produce a fairly uniform beam from the ion source (a Gaussian density distribution with $\sigma = \sqrt{2}$). Since the aberrations produced by the Pierce geometry are very small in this case it is preferable to employ such a structure so as to keep the beam divergence and radius to a minimum when it enters the triplet.

Aknowledgements

The author wishes to thank M. Weiss and L.R. Evans, Linac Group, CERN, for much helpful discussion and advice, and C.S. Taylor, Linac Group, CERN, for his help and encouragement at all stages of this work.

References

1.   A.J. Davies, 1970, The Transverse Motion of Rotationally Symmetric Charged Particle Beams. Nuclear Instruments and Methods, 80 , 45 - 54.

2.   J.R. Pierce, 1954, Theory and Design of Electron Beams, (London : Van Nostrand).

3.   See section on GD3 package, CERN Programme Library.

4.   C.S. Taylor, 1969, Non-Linear Space Charge Effects in Non-Uniform Beams, MPS/Int. LIN 69-14.
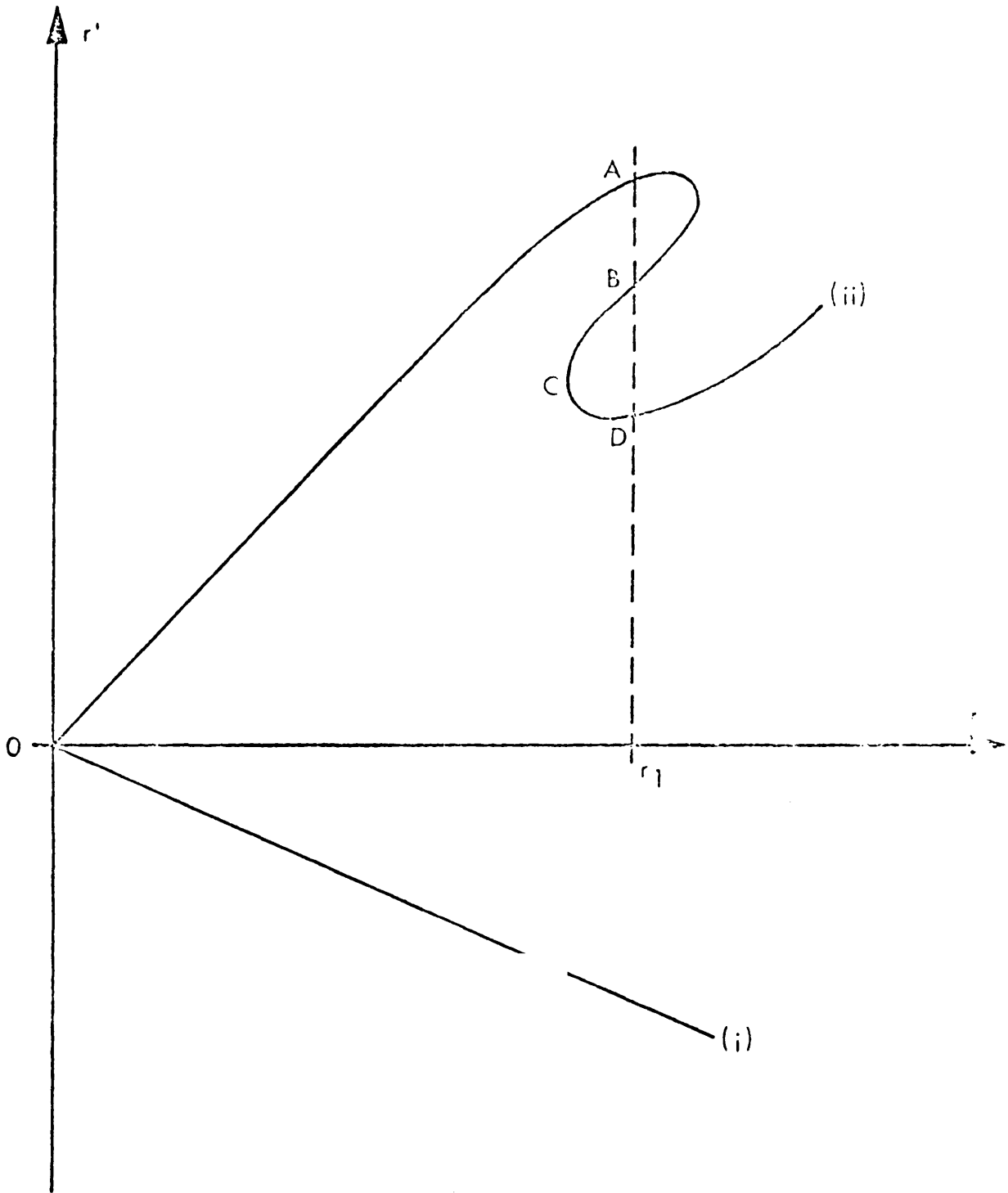
Distribution   (open)

Fig. 1. (i) Initial position of zero emittance line and
(ii) typical shape of line at subsequent time.

Fig. 2. Particle trajectories in a uniform beam subject to a linear focusing field of 267r volts/cm. Beam current 0.1 A; energy 750 keV.
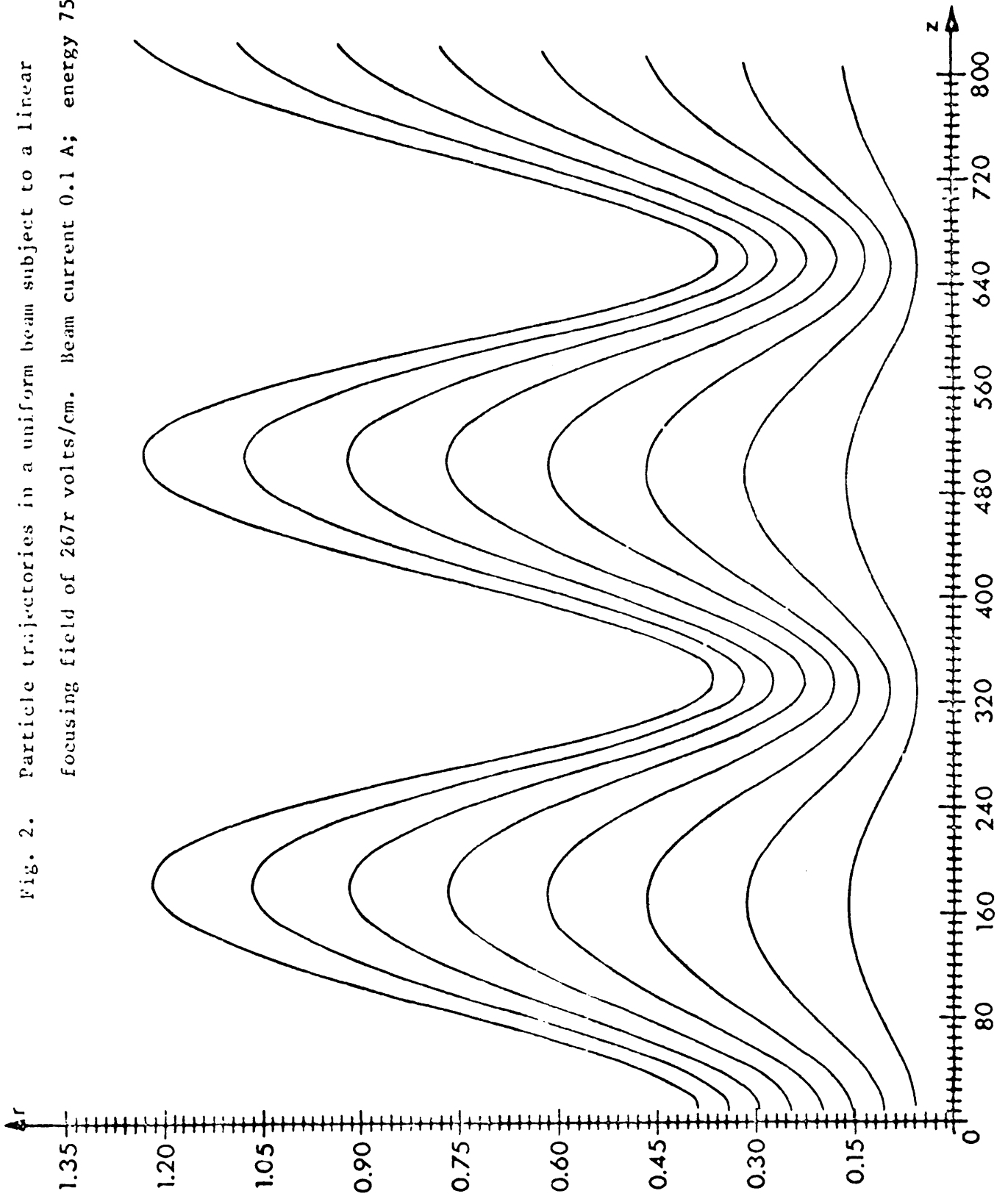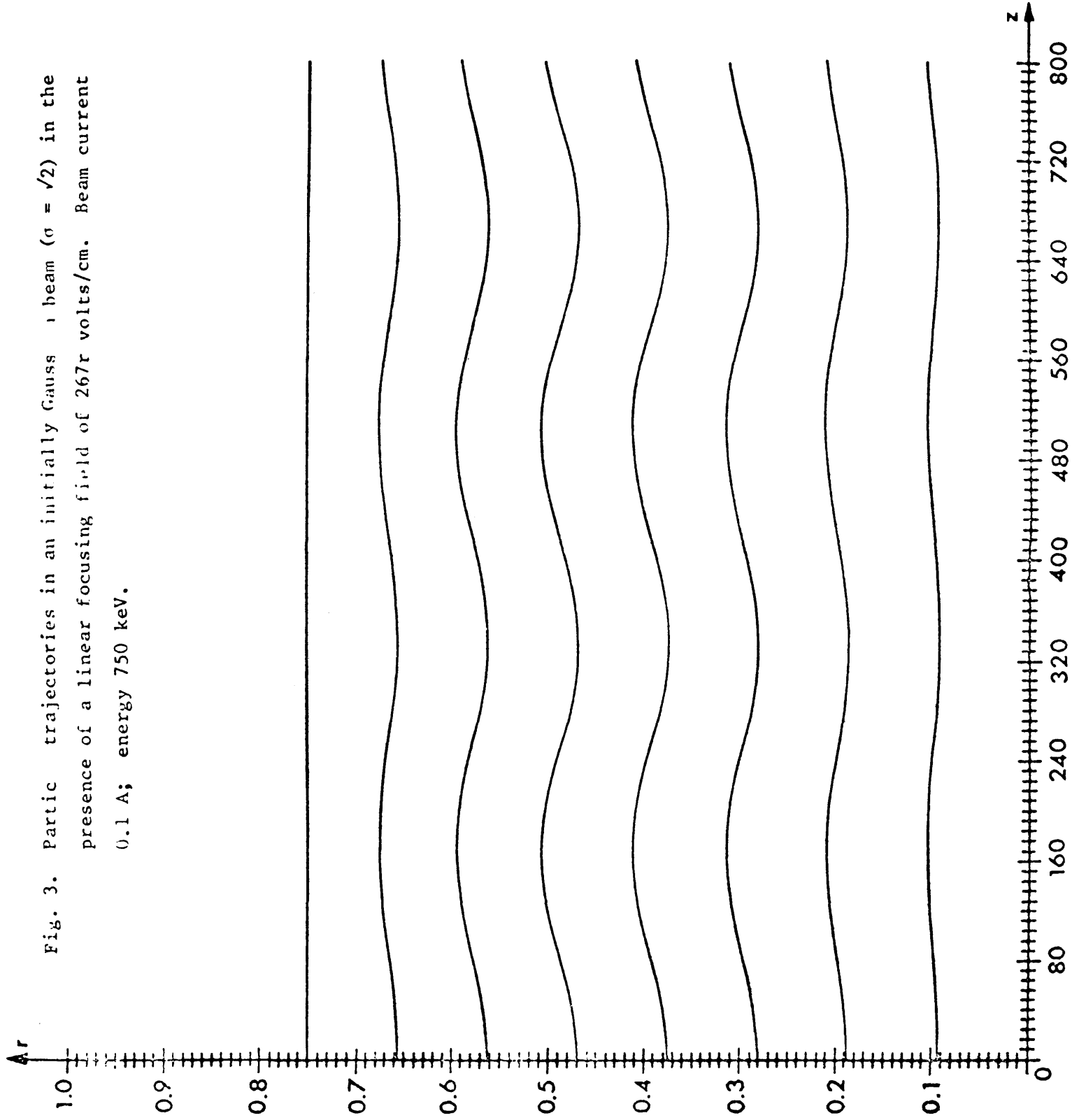
Fig. 3. Particle trajectories in an initially Gaussian beam ($\sigma = \sqrt{2}$) in the presence of a linear focusing field of 267r volts/cm. Beam current 0.1 A; energy 750 keV.
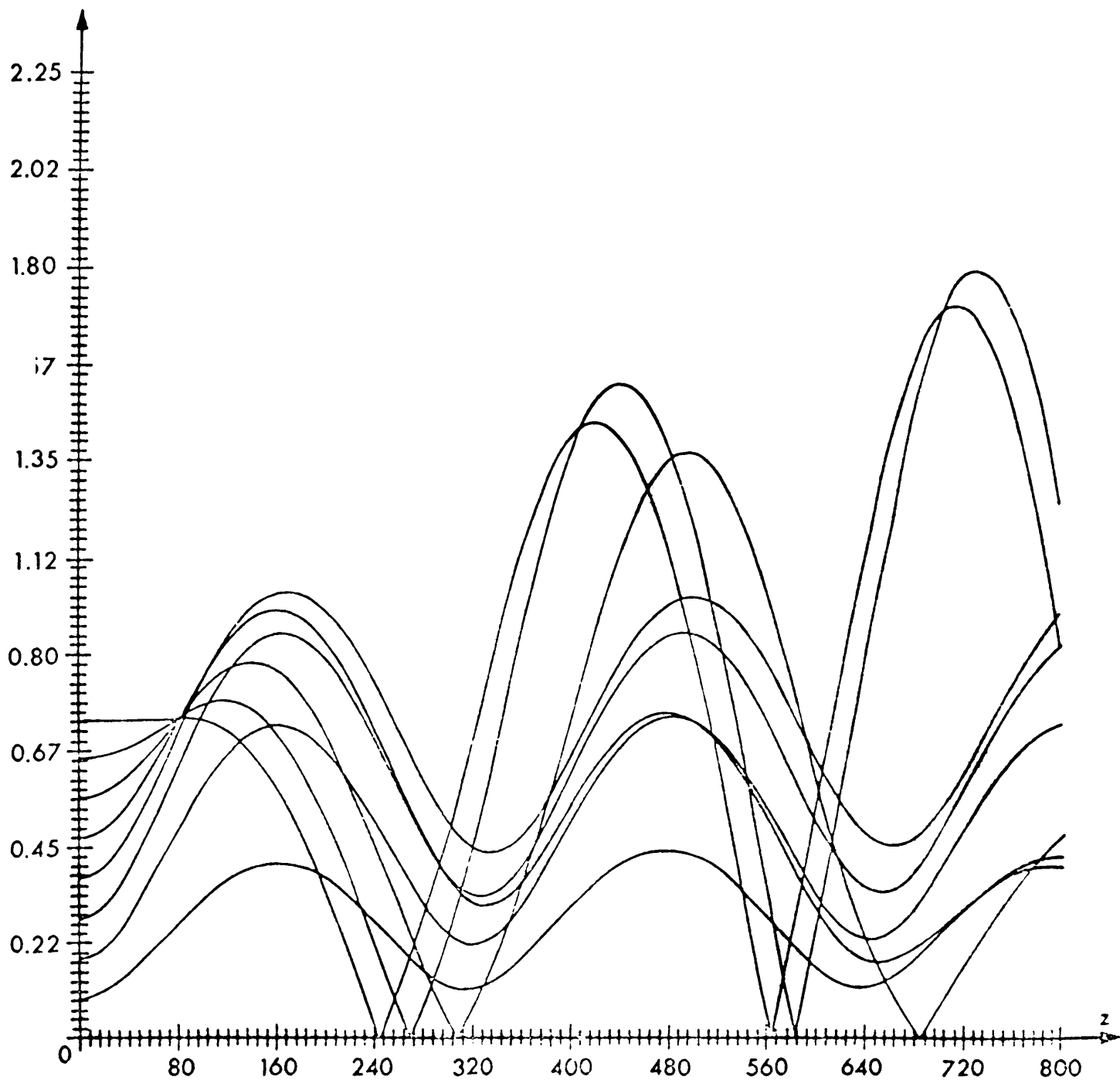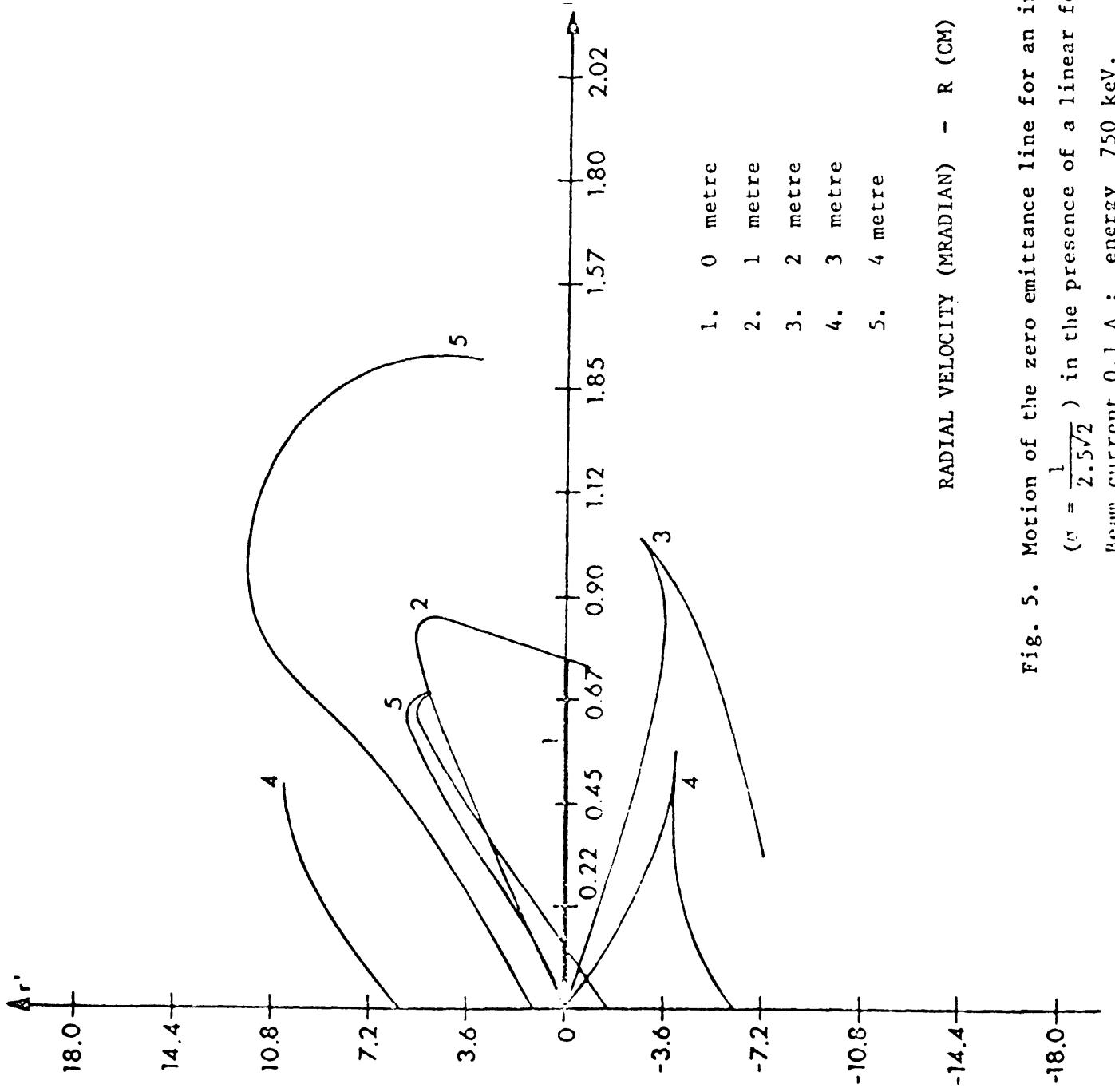
Fig. 4. Particle trajectories in an initially Gaussian beam ($= \dfrac{1}{2.5\ \sqrt{2}}$)
in the presence of a linear focusing field of 267r volts/cm.
Beam current 0.1 A;   energy   750 keV.

RADIAL VELOCITY (MRADIAN) — R (CM)

1. 0 metre
2. 1 metre
3. 2 metre
4. 3 metre
5. 4 metre

Fig. 5. Motion of the zero emittance line for an initially Gaussian beam $(\sigma = \frac{1}{2.5\sqrt{2}})$ in the presence of a linear focusing field of $267r$ volts/cm. Beam current 0.1 A; energy 750 keV.
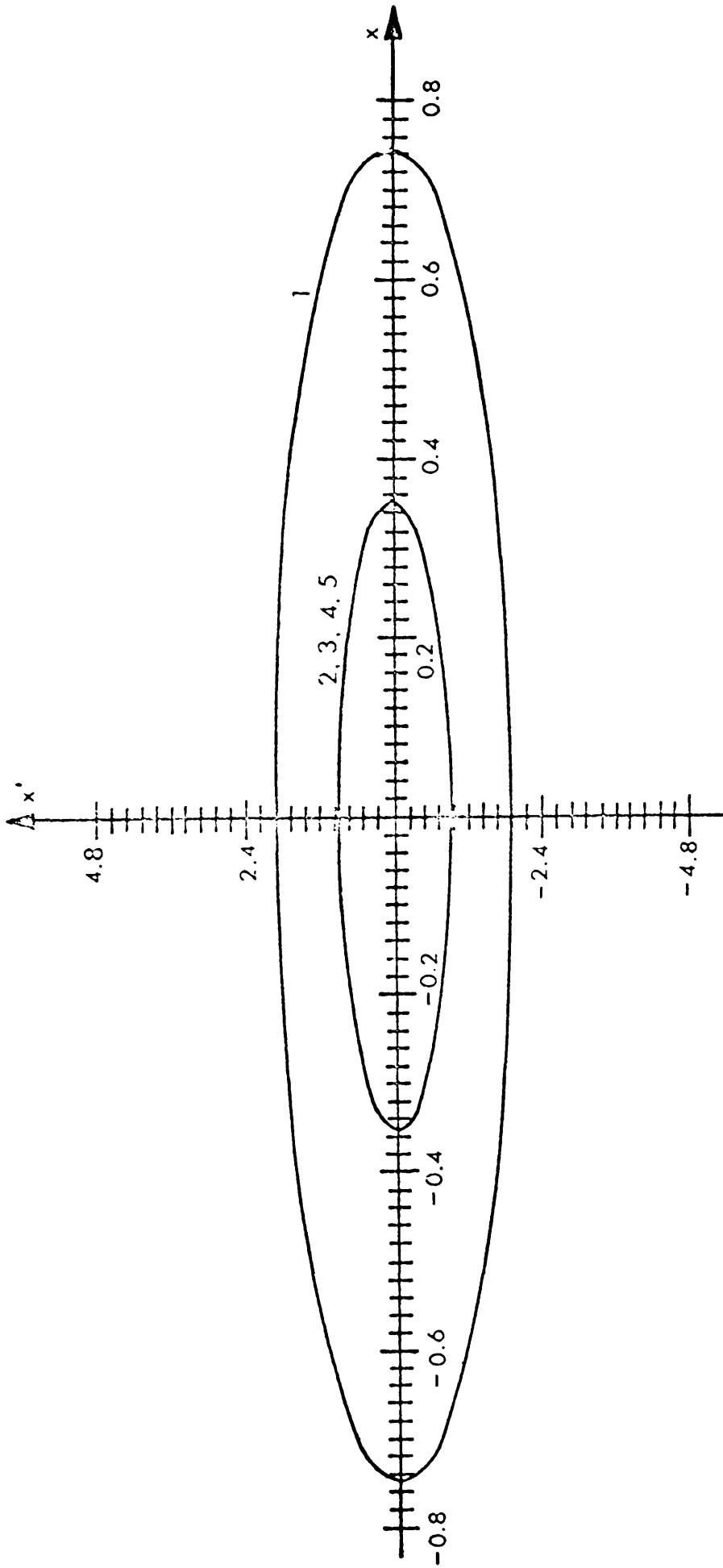
1. Beam boundary in xx' plane (eqn(10)); $y = y' = 0$.

2. 50% contour in xx' plane (eqn(11)); $y = y' = 0$.

3. Projection of section defined by (13); $y = 0$, $y' = b \sqrt{1 - \frac{1}{k^2}}$

4. Projection of section defined by (14); $y = \frac{a}{2} \sqrt{1 - \frac{1}{k^2}}$, $y' = \sqrt{\frac{3}{4}} \cdot b \cdot \sqrt{1 - \frac{1}{k^2}}$

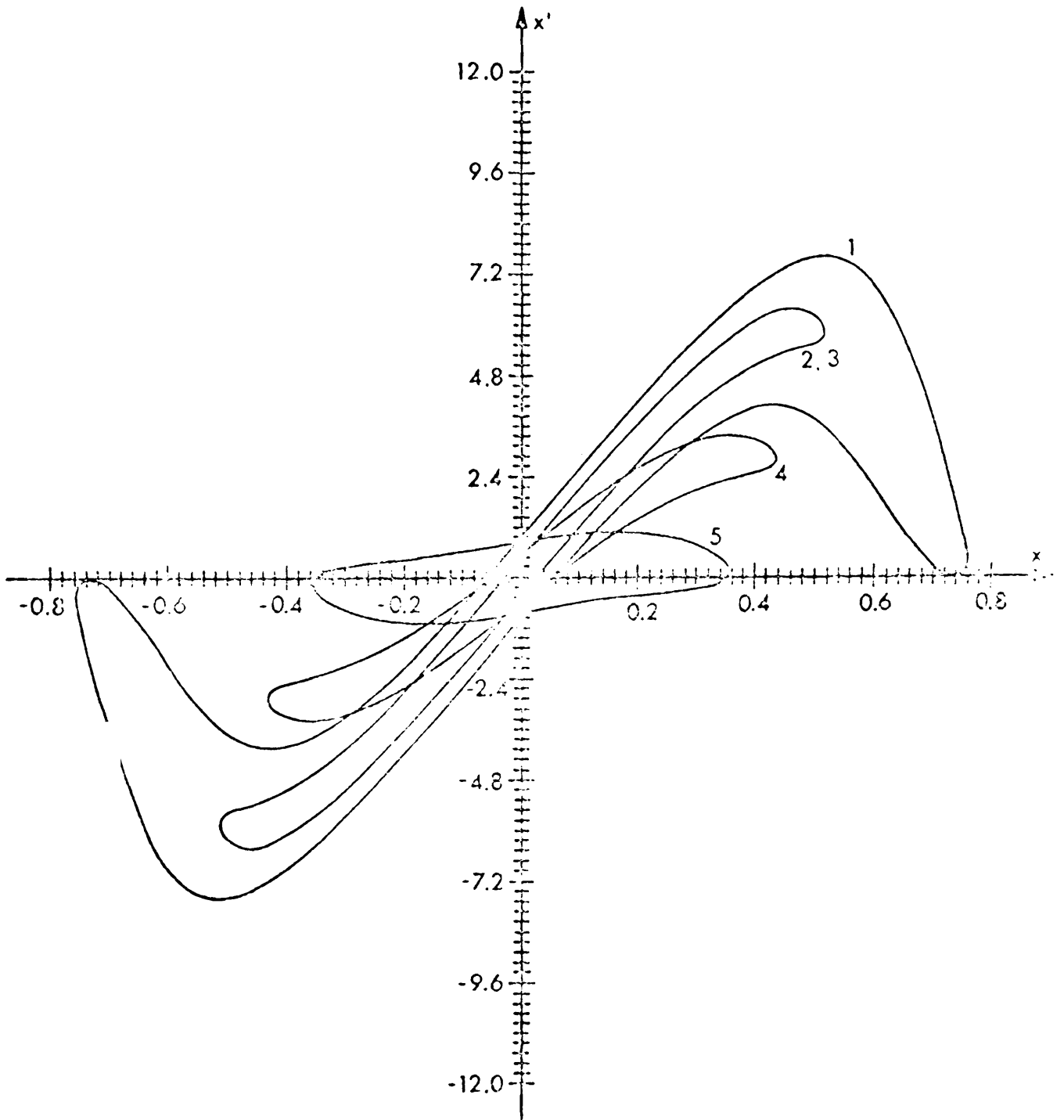5. Projection of section defined by (12); $y = a \sqrt{1 - \frac{1}{k^2}}$, $y' = 0$

Fig. 6. Initial positions of (10) to (14) in xx' plane. Beam current 0.1 A; energy 750 keV. Gaussian distribution $\sigma = \frac{1}{2.5 \sqrt{2}}$
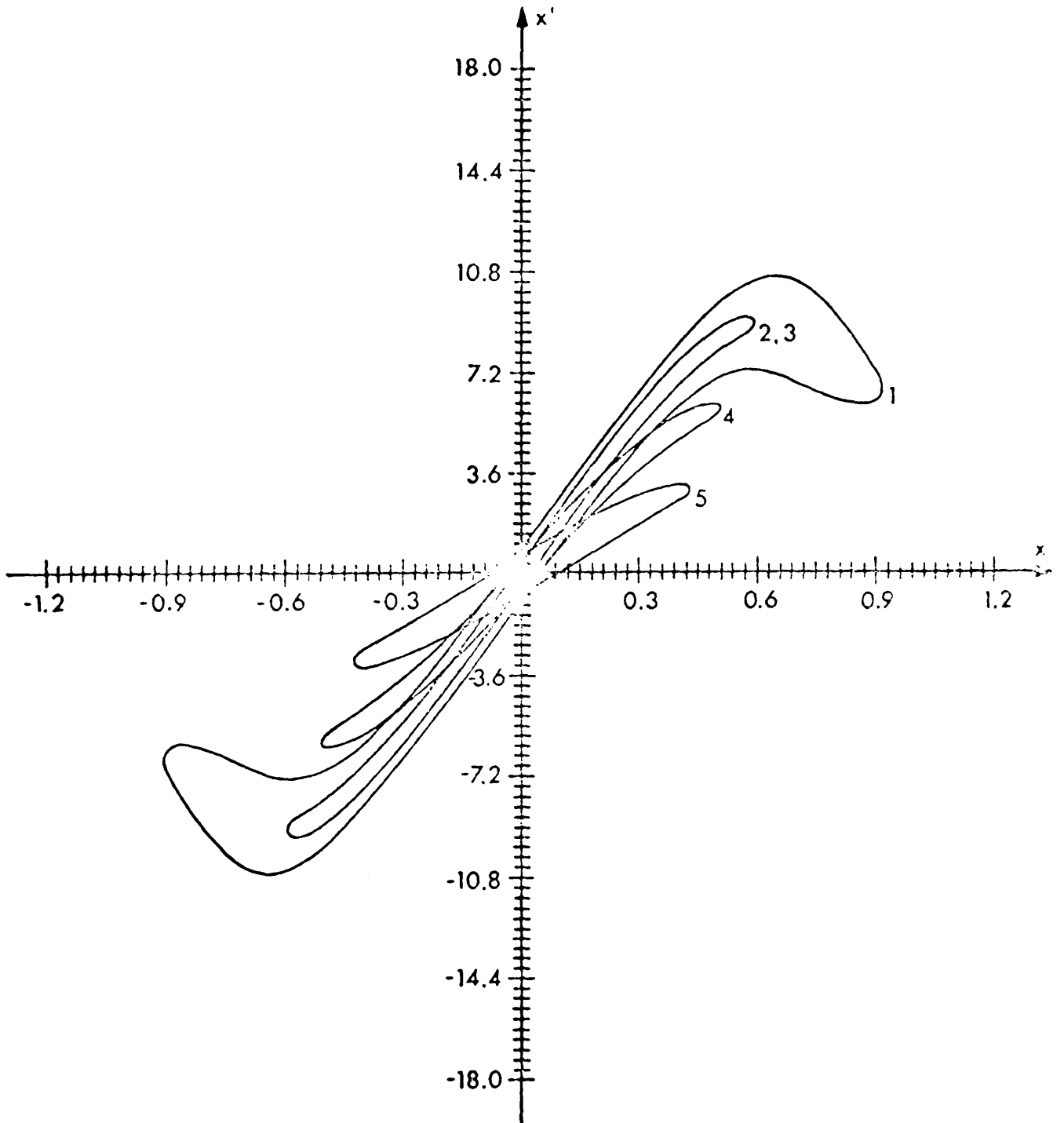
VELOCITY X' (MRADIAN) - X (CM)

Fig. 7. Positions of curves 1. to 5. of Fig. 6 after 50 cm drift.

VELOCITY X' (MRADIAN) - X (CM)

Fi.g 8.   Positions of curves 1. to 5. of Fig. 6 after 50 cm drift with
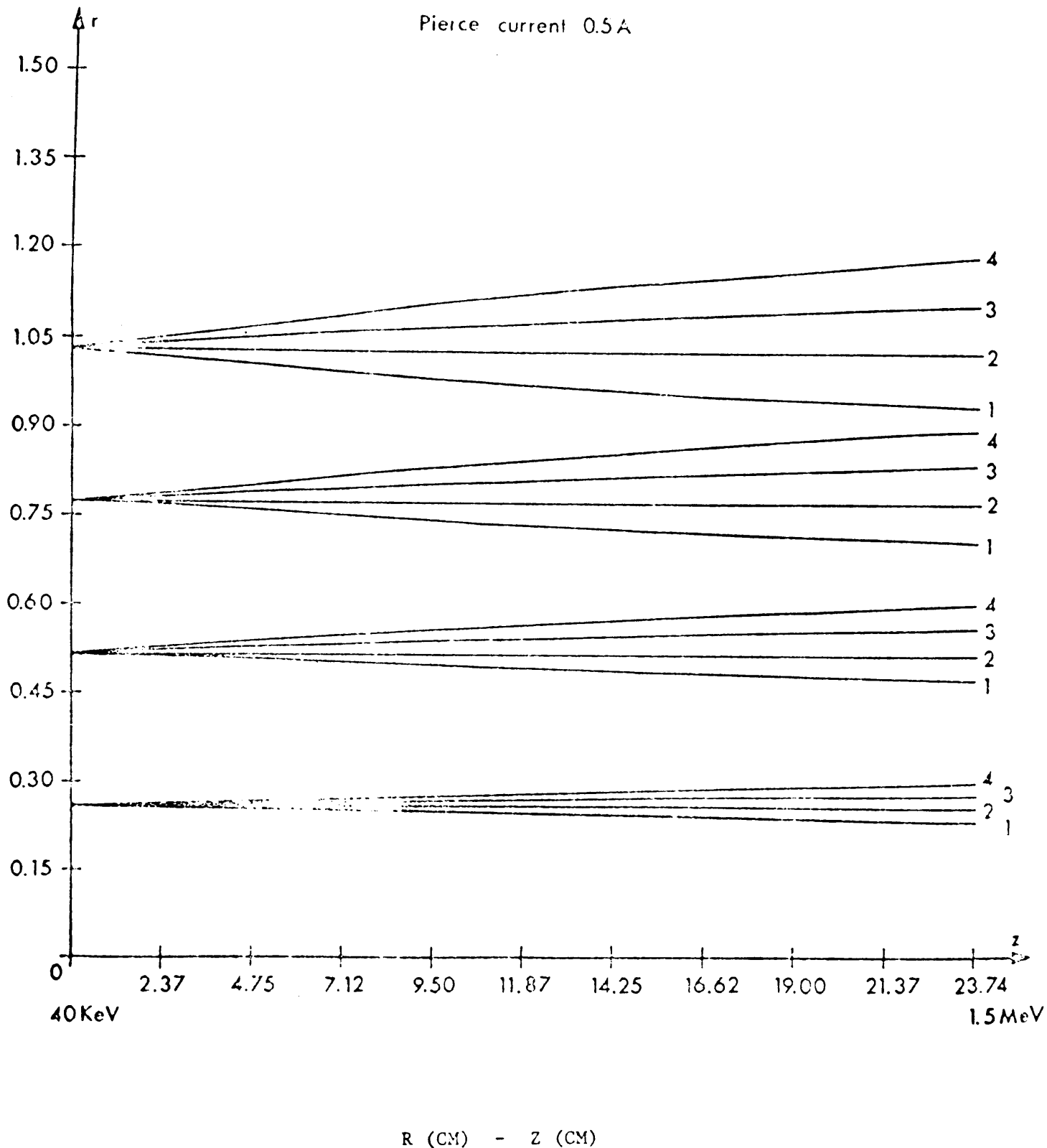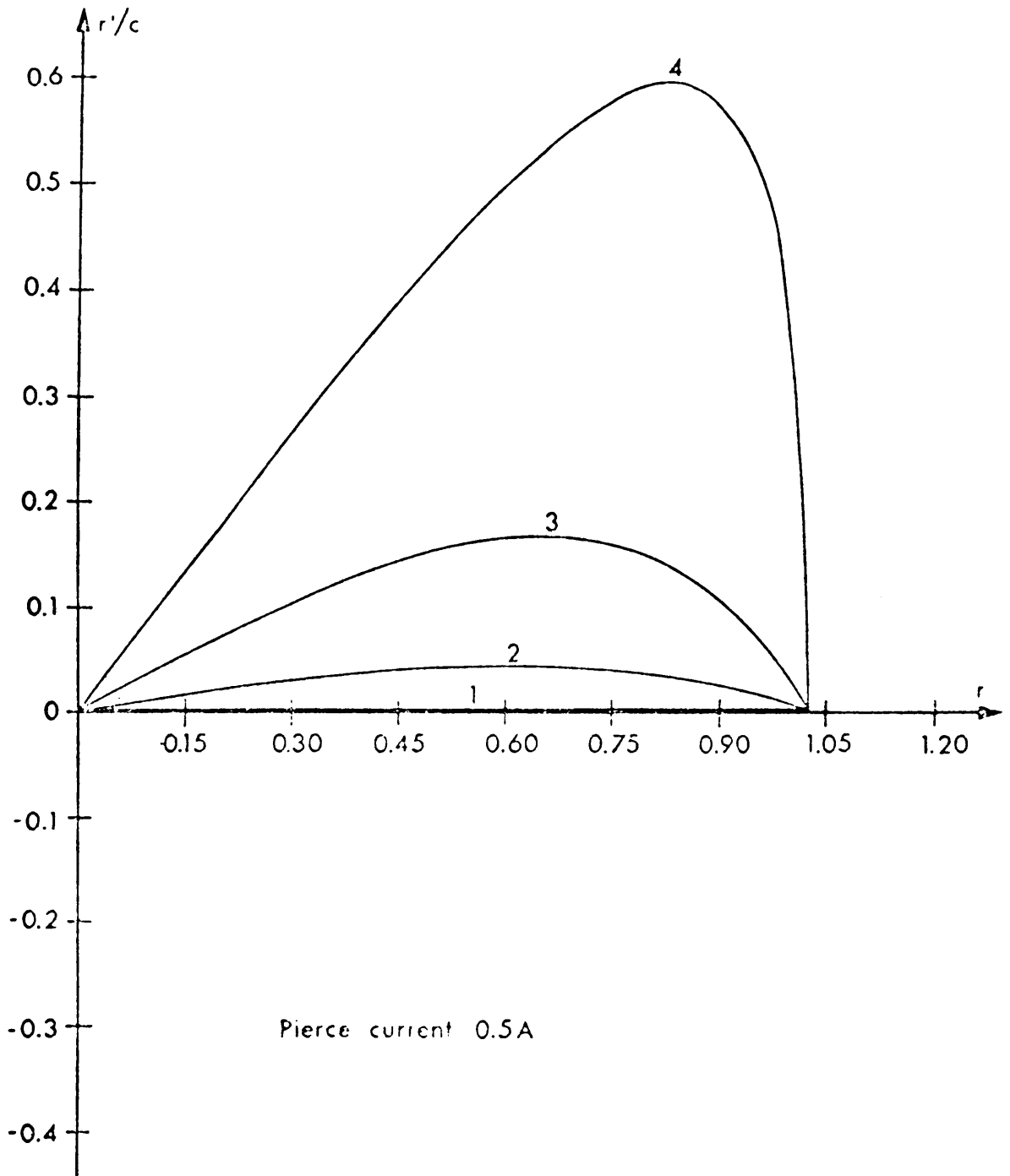linear focusing field of 267r volts/cm.

Fig. 9. Particle trajectories in uniform proton beams accelerated from 40 keV
to 1.5 MeV in a Pierce structure designed for 0.5 A. Beam currents :
1. 0.417 A ; 2. 0.5 A ; 3. 0.583 A ; 4. 0.667 A.

RADIAL VELOCITY/C (MRADIAN) - R(CM)

Fig. 10. Zero emittance lines after acceleration from 40 keV to 1.5 MeV in a Pierce system. Beam current 0.5 A. Initial distribution Gaussian :
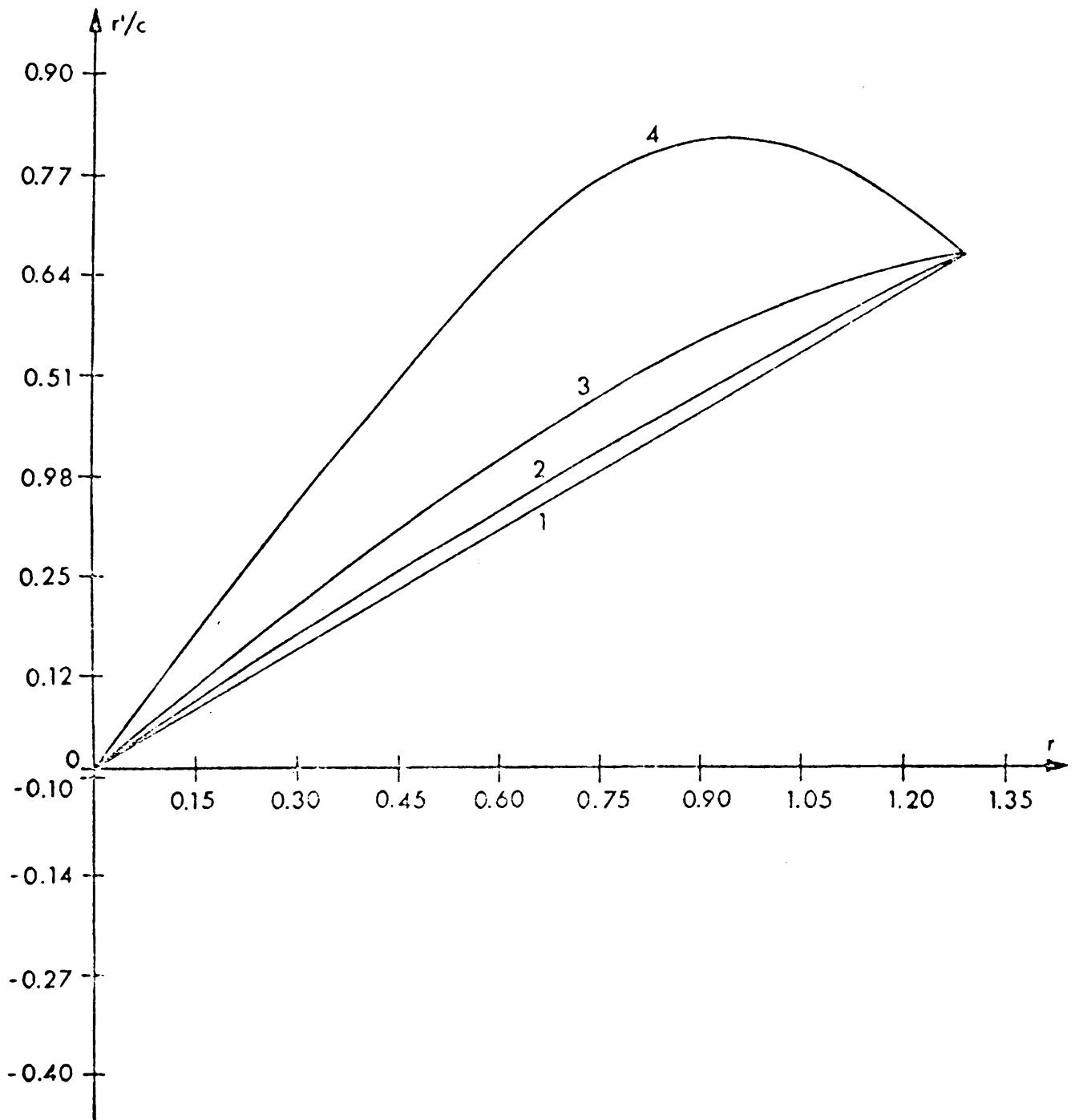
1. $\sigma = 0$ 2. $\sigma = 2$ 3. $\sigma = \dfrac{1}{\sqrt{2}}$ 4. $\sigma = \dfrac{1}{2\sqrt{2}}$

RADIAL VELOCITY/C (MRADIAN) - R (CM)

Fig. 11 Zero emittance lines after acceleration from 40 keV to 1.5 MeV at a gradient of 7.6 MeV/metre. Beam current 0.5 A. Initial distribution Gaussian : 1. $\sigma = 0$ 2. $\sigma = \sqrt{2}$ 3. $\sigma = \dfrac{1}{\sqrt{2}}$ 4. $\sigma = \dfrac{1}{2\sqrt{2}}$